

Synthesis and Electrical Characterization of Cu^{2+} doped $(\text{SnO}_2)_{1-x}(\text{ZnO})_x$ nanocomposites.

K.J.Abhirama*, K.U.Madhu *

*Physics Research Centre, S.T.Hindu College, Nagercoil– 629002,

(Affiliated to Manonmaniam Sundaranar University, Tirunelveli)Tamil Nadu, India.

ABSTRACT

$(\text{SnO}_2)_{1-x}(\text{ZnO})_x$ (with x values 0.0,0.2,0.4,0.5,0.6,0.8,1.0) nanocomposites doped with 1 mole percent Cu^{2+} was synthesized using simple microwave assisted solvothermal method with ethylene glycol as solvent. The as-prepared samples were calcinated for about 500°C and the calcinated samples were characterized using powder X-ray diffraction analysis (PXRD) and the electrical measurements were carried out within the temperature range of $40\text{-}150^\circ\text{C}$. The electrical parameters such as dielectric constant and dielectric loss factor were found to increase with increase in temperature and decreases with increase in frequency. The occurrence of space charge polarization was responsible for the changes. It was observed that the AC electrical conductivity increases with increase in frequency and temperature and it was mainly due to hopping of electrons. The results obtained were reported and discussed.

Keywords: Calcinated, Conductivity, Dielectric parameters, Nanocomposite, Solvothermal.

Date of Submission: 21-11-2017

Date of acceptance: 30-11-2017

I. INTRODUCTION:

In recent years, studies on ZnO, SnO_2 nanoparticles and their composites are increasing due to their interesting properties and applications in various fields like optoelectronic devices, solar cell, sensor, lithium-ion batteries and so on [1-6]. SnO_2 and ZnO are n-type semiconducting materials with a wide band gap of 3.6-3.8eV and 3.37eV respectively and they are considered as a suitable material for dye-sensitized solar cell [7-10]. ZnO/ SnO_2 composite is capable of enhancing the gas sensing ability and the optical properties [11]. Addition of dopant affects the dielectric properties of parent material [12-14]. Enhancement in the dielectric properties of SnO_2 nanowires in the low frequency range was reported by Babar et al [15]. Various synthesis techniques like sol gel method, pulsed laser deposition, liquid phase plasma method, emulsion techniques, solvothermal method, spray pyrolysis, sonochemical, spark

plasma sintering, hydrothermal, microwave assisted method chemical precipitation method and co-precipitation method are employed for the preparation of SnO_2 , ZnO and their composite nanomaterials [16-32].

Abhirama et al have synthesized and carried out the electrical characterization of $(\text{SnO}_2)_{1-x}(\text{ZnO})_x$ nanocomposites [33]. The present work deals with the synthesis of Cu^{2+} doped $(\text{SnO}_2)_{1-x}(\text{ZnO})_x$ (with x values 0.0,0.2,0.4,0.5,0.6,0.8,1.0) nanocomposite using a simple microwave assisted solvothermal method. Ethylene glycol was used as solvent for the preparation of Cu^{2+} doped $(\text{SnO}_2)_{1-x}(\text{ZnO})_x$ (with x values 0.0,0.2,0.4,0.5,0.6,0.8,1.0) nanocomposite. The as-prepared samples were calcinated at 500°C and the samples were characterized using PXRD and the electrical parameters were studied using the pellets of calcinated nanocomposites. The results obtained are reported and discussed.

II. EXPERIMENT AND CHARACTERIZATION:

Analytical grade copper acetate, stannous chloride dehydrate, zinc acetate dehydrate, urea and ethylene glycol were used for the preparation of Cu^{2+} doped $(\text{SnO}_2)_{1-x}(\text{ZnO})_x$ (with x values 0.0,0.2,0.4,0.5,0.6,0.8,1.0) nanocomposite. Cu^{2+} doped SnO_2 (when $x=0$) nanoparticles were synthesized by taking 1 mole percent of copper acetate along with stannous chloride and urea in

1:3 molecular ratio. Solution of copper acetate, stannous chloride and urea were obtained by dissolving them separately in 200 ml ethylene glycol solution with the help of a magnetic stirrer. Into the stannous chloride solution which was kept under stirring the urea solution was added dropwise and at last the copper acetate solution was added. Then the solution obtained was kept in a domestic microwave oven (operated with a frequency of 2.5 GHz and power 800 W). The

solvent in the solution gets evaporated when it was irradiated with microwave radiation and a colloidal precipitate was formed. The colloidal precipitate was washed with double distilled water for five times and then with acetone in order to eliminate the organic impurities present if any. Then the washed samples were desiccated in atmospheric air and it is collected as yield and preserved. Similar procedure and molecular ratio was followed to synthesis Cu^{2+} doped ZnO (when $x=1$) nanoparticles and composites of $(\text{SnO}_2)_{1-x}(\text{ZnO})_x$ (with $x = 0.2, 0.4, 0.5, 0.6, 0.8$). The only difference is in the precursors used. Cu^{2+} doped ZnO (when $x=1$) nanoparticles were prepared by taking copper acetate, zinc acetate and urea. The composites of Cu^{2+} doped $(\text{SnO}_2)_{1-x}(\text{ZnO})_x$ (with $x = 0.2, 0.4, 0.5, 0.6, 0.8$) were prepared by taking copper acetate, stannous chloride, zinc acetate and urea.

Cu^{2+} doped $(\text{SnO}_2)_{1-x}(\text{ZnO})_x$ (with x values 0.0, 0.2, 0.4, 0.5, 0.6, 0.8, 1.0) nanocomposite annealed at 500°C were characterized by powder X-ray diffractometer (XPRT-PRO) using $\text{Cu K}\alpha$ ($\lambda=1.54060$ AU) radiation. The electrical parameters of calcinated samples were analyzed using Agilent LCR meter in the temperature range of $40\text{-}150^\circ\text{C}$. For the electrical measurements the powdered samples were pelletized using a hydraulic press and these pellets were used to carry out the measurements. For the good conductivity of the pellets the flat surfaces of it was coated with graphite. The electrical measurements were made while cooling.

III. RESULT AND DISCUSSION

(3.1) XRD ANALYSIS

Figure (1) shows the PXRD pattern of calcinated Cu^{2+} doped $(\text{SnO}_2)_{1-x}(\text{ZnO})_x$ (with x values 0.0, 0.2, 0.4, 0.5, 0.6, 0.8, 1.0) nanocomposite. The diffraction peaks obtained in the spectra corresponding to the x values (0.0 and 1.0) was in agreement with the tetragonal phase of SnO_2 with lattice constants $a = 4.7448$ and $c = 3.1932$ (PDF number: 88-0287) and hexagonal phase of ZnO with lattice constants $a = 3.2519$ and $c = 5.2059$ (PDF number: 89-1397). The diffraction peaks obtained in the spectra corresponding to the x values (0.2, 0.4, 0.5, 0.6, and 0.8) contains SnO_2 and ZnO phases. No peaks corresponding to copper are detected in the PXRD pattern of Cu^{2+} doped $(\text{SnO}_2)_{1-x}(\text{ZnO})_x$ [with x values 0.0, 0.2, 0.4, 0.5, 0.6, 0.8, 1.0] nanocomposites because only a few amount of copper acetate was added as the dopant. Also the Cu ions are incorporated into the lattice of the host material [24]. A slight shift in the diffraction peak towards the lower angle was observed. There was no mark out of other phases or diffraction patterns analogous to SnO , ZnSnO_3 , ZnSnO_4 . Similar result was already reported by Neha et al [6] and Omar et al [34]. The broadening of peaks in the XRD pattern of Cu^{2+} doped $(\text{SnO}_2)_{1-x}(\text{ZnO})_x$ nanocomposites indicates the nanocrystalline nature of the samples. The average crystalline size was calculated using Debye-Scherer formula [30] and it was found to be 11-36nm.

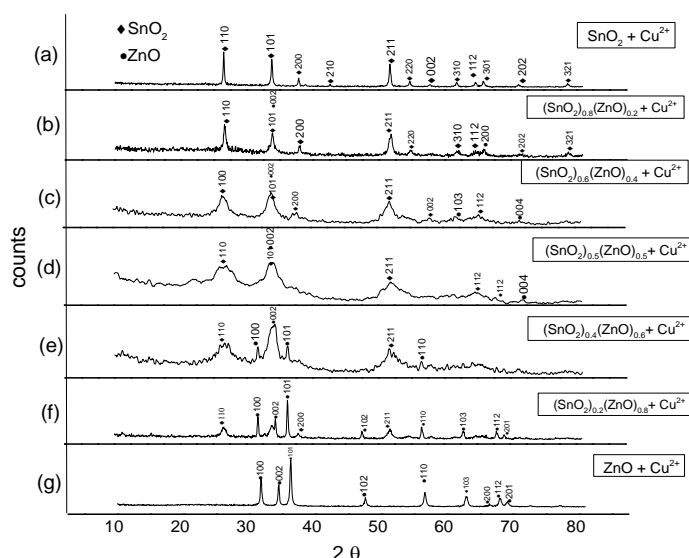


Figure 1: The PXRD pattern of Cu^{2+} doped $(\text{SnO}_2)_{1-x}(\text{ZnO})_x$ nanocomposites.

(3.2) Electrical Parameters

Figure 2-22 shows the behaviour of electrical parameters such as dielectric constant, dielectric loss factor and the AC electrical conductivity of all the samples with respect to

temperature and frequency. The dielectric constants was calculated using the relation $\epsilon_r = C/C_0$. The AC electrical conductivity (σ_{ac}) was calculated using the formula:

$$\sigma_{ac} = \epsilon_0 \epsilon_r \omega \tan \delta.$$

Where ϵ_0 is the permittivity of free space ($8.85 \times 10^{-12} \text{ C}^2\text{N}^{-1}\text{m}^{-2}$) and ω is the angular frequency ($\omega = 2\pi f$, where f is the frequency). Figure 2-8 shows the variation of dielectric constant with frequency and temperature. It was observed that the dielectric constant value increases with increase in temperature while it decreases with increase in frequency. The space charge polarization was predominant in heterogeneous structures and it results in the decrease of dielectric constant with increase in frequency [14]. In Cu^{2+} doped $(\text{SnO}_2)_{1-x}(\text{ZnO})_x$ nanocomposites at low frequency the value of dielectric constant for the end members was less when compared to that for the composites.

At low temperatures the charge carriers have low thermal energy and it cannot follow electric field direction and hence the dielectric constant value is low. Thus in polarization mechanism the contribution of charge carriers at low temperatures are minimum. While at high temperatures the charge carriers possess enough thermal energy and hence it respond to the change in external field [35].

Figure: 2-8 shows the variation of dielectric constant with frequency and temperature for Cu^{2+} doped $(\text{SnO}_2)_{1-x}(\text{ZnO})_x$ nanocomposites.

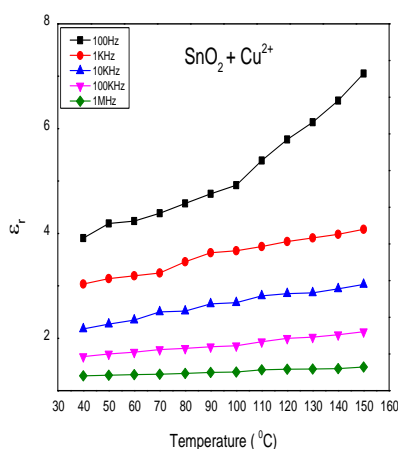


Figure: 2

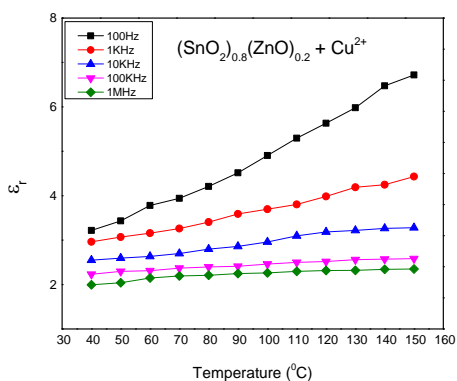


Figure: 3

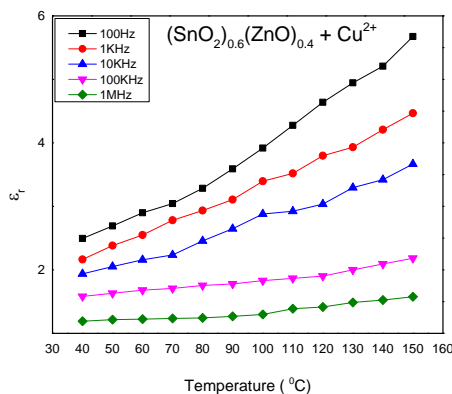


Figure: 4

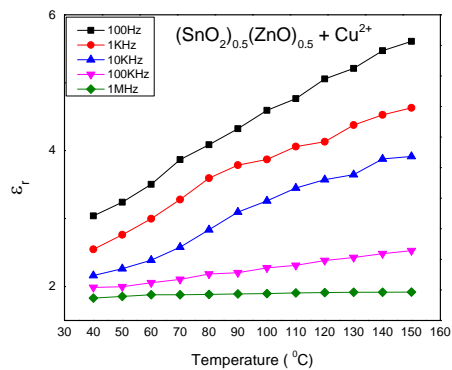


Figure: 5

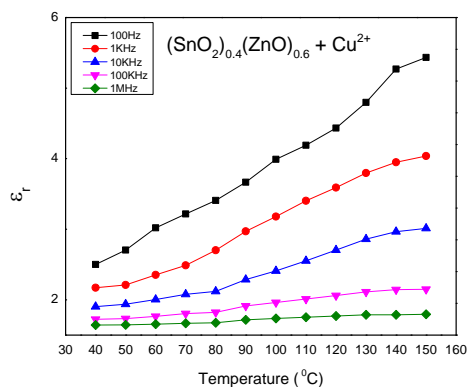


Figure:6

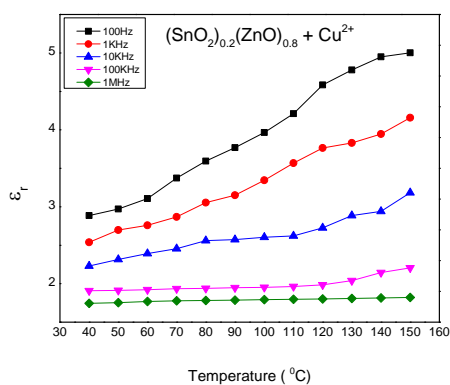


Figure:7

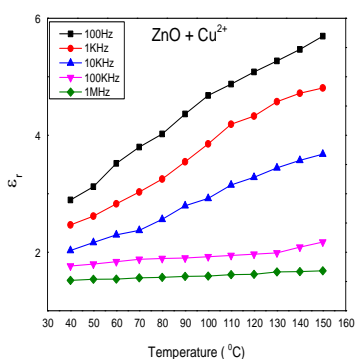


Figure: 8

In Cu^{2+} doped $(\text{SnO}_2)_{1-x}(\text{ZnO})_x$ nanocomposites for lower frequencies low value of dielectric loss factor was observed for the end members than that for the composites. For higher frequencies and temperature the value of dielectric loss factor was high for the composites than that for the end members except the composite with x values (0.6, 0.8). It was observed that the dielectric loss factor increases with increase in temperature and decreases with increase in frequency. Dipoles remain fixed at lower temperatures while they are free to move at higher temperatures and hence it can respond to the applied electric field. Thus an increase in dielectric constant and dielectric loss factor was observed with increase in temperature.

Figure: 9-15 shows the variation of dielectric loss factor with frequency and temperature for Cu^{2+} doped $(\text{SnO}_2)_{1-x}(\text{ZnO})_x$ nanocomposites.

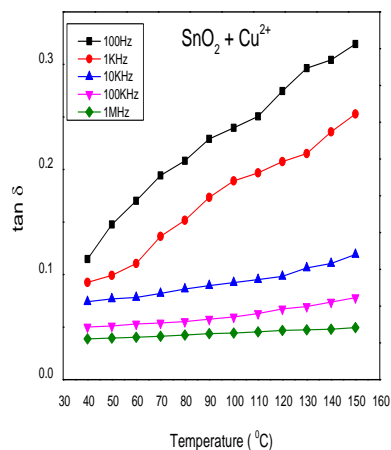


Figure: 9

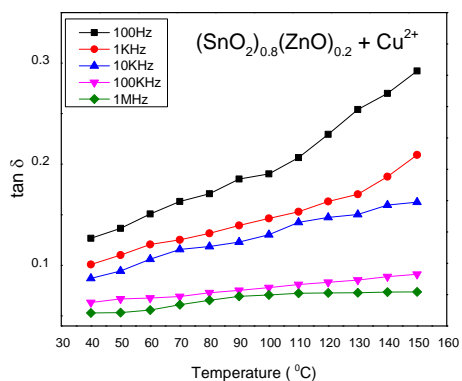


Figure: 10

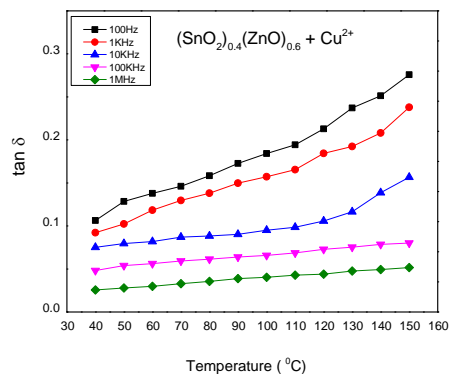


Figure: 13

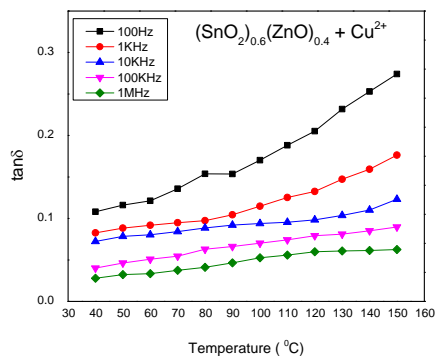


Figure: 11

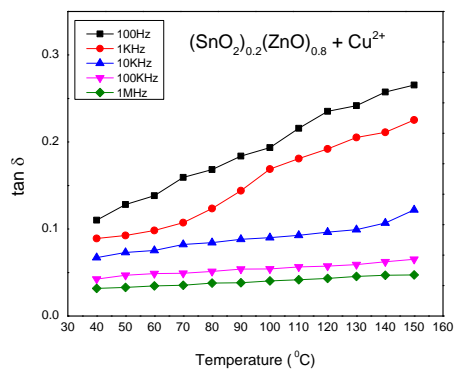


Figure: 14

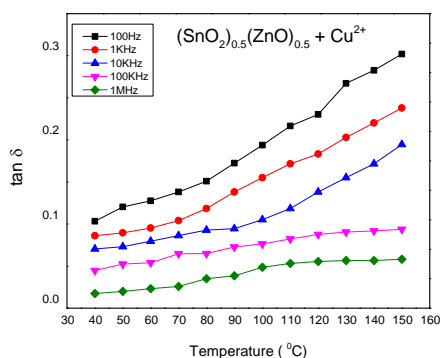


Figure: 12

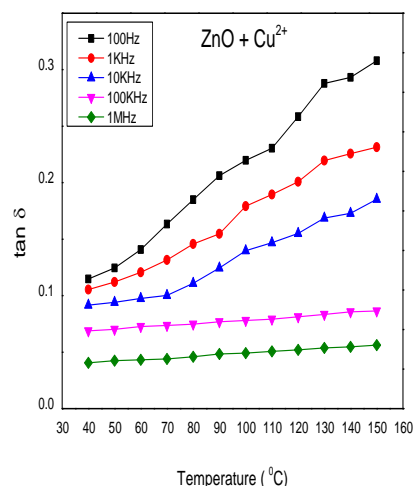


Figure: 15

It was observed that for all the prepared samples the AC electrical conductivity increases with increase in temperature and frequency. Here the AC electrical conductivity increases with frequency and hence the mechanism of conduction in the prepared samples is

localized conduction mechanism [36]. Also the conduction process was due to small polaron hopping since the conductivity increases with frequency [15].

In Cu^{2+} doped $(\text{SnO}_2)_{1-x}(\text{ZnO})_x$ nanocomposites at low frequencies the value of AC electrical conductivity for the end members was high when compared to that for the composites. For higher frequencies and temperature the value of AC electrical conductivity was higher for the composites than that for the end members except the composite with x values (0.6, 0.8). The electronic polarization occurs due to hopping of electrons and

the hopping is due to the mobility of charge carriers hence AC electrical conductivity increases with increase in temperature. At the interfaces the defects such as vacancy clusters, microporosites and dangling bonds causes change of positive and negative space charge distributions. When these charge distributions are trapped at the defect sites dipole moments are produced and it results in the occurrence of space charge polarization [37].

Figure: 16-22 shows the variation of AC electrical conductivity with frequency and temperature for Cu^{2+} doped $(\text{SnO}_2)_{1-x}(\text{ZnO})_x$ nanocomposites.

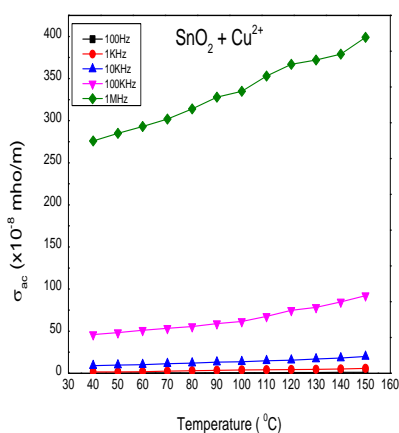


Figure: 16

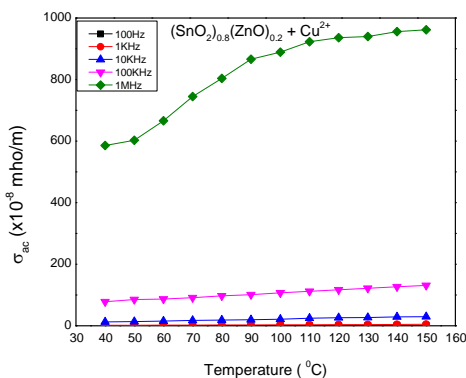


Figure: 17

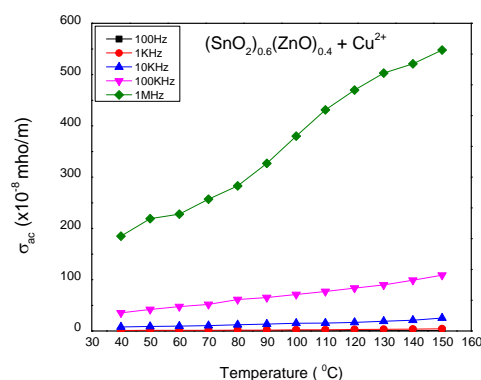


Figure: 18

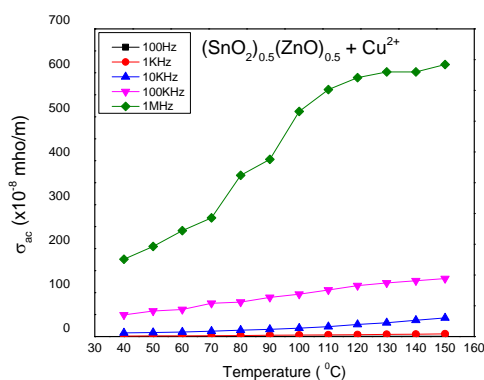


Figure: 19

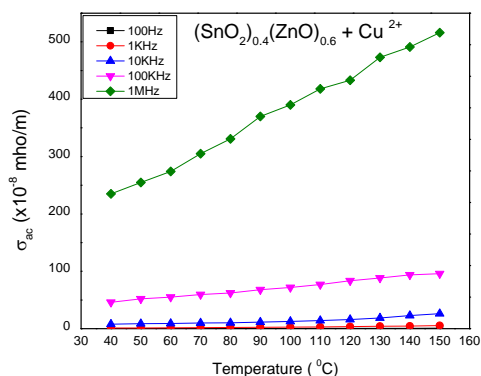


Figure: 20

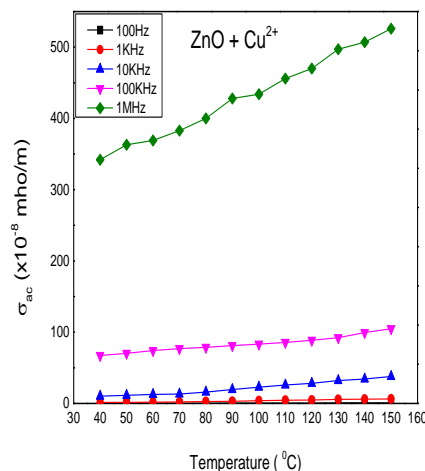


Figure: 22

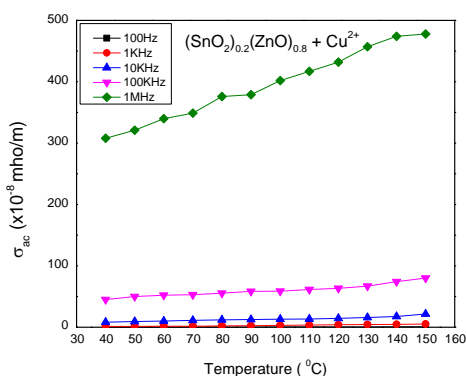


Figure: 21

IV. CONCLUSION

A simple microwave assisted solvothermal method was chosen for the preparation of Cu^{2+} doped $(\text{SnO}_2)_{1-x}(\text{ZnO})_x$ (with x values 0,0.2,0.4,0.5,0.6,0.8,1) nanocomposite using ethylene glycol as solvent. The average particle size was calculated as 11- 36nm. The dielectric loss factor and dielectric constant decreases with increase in frequency and increases with increase in temperature. The space charge polarization causes decrease in dielectric loss factor and dielectric constant with increase in frequency. Increase in AC electrical conductivity with increase in frequency and temperature was noted and it was due to hopping of electrons. The mechanism of conduction in the prepared samples is localized conduction mechanism. Also the conduction process was due to small polaron hopping.

REFERENCES

- [1]. Jun Song Chen and Xiong Wen (David) Lou SnO_2 and TiO_2 nanosheets for lithium-ion batteries, *Materials today*, vol 15, No 6, (2012), 246-254.
- [2]. N.D. Md Sin, M.Z. Musa, M.H. Mamat, S.Ahmad, Abdul Aziz. A and M. Rusop, Zinc Oxide Buffer Layer Insertion for Sensitivity Improvement in Aluminium-Doped Zinc Oxide-Based Humidity Sensors, *Advanced Materials Research*, Vol. 667, (2013), 287-293.
- [3]. Franziska Mueller, Dominic Bresser, Venkata Sai Kiran Chakravadhanula, Stefano Passerini, Fe-doped SnO_2 nanoparticles as new high capacity anode material for secondary lithium-ion batteries, *Journal of Power Sources*, 299, (2015), 398-402.
- [4]. Kuo-YuanHwa, Boopathi Subramani, Synthesis of zinc oxide nanoparticles on graphene-carbon nanotube hybrid for glucose biosensor applications, *Biosensors and Bioelectronics*, 62, (2014), 127-133.
- [5]. Suresh Kumar, Ravi Nigam, Virender Kundu, Neena Jaggi, Sol-gel synthesis of ZnO-SnO_2 nanocomposites and their morphological, structural and optical properties, *J Mater Sci: Mater Electron*, (2015), 7 pages.
- [6]. Neha Bhardwaj, Sini Kuriakose, A. Pandey, R.C. Sharma, D.K. Avasthi, Satyabrata Mohapatra, Effects of MeV ion irradiation on structural and optical properties of $\text{SnO}_2\text{-ZnO}$ nanocomposites prepared by

- carbothermal evaporation, *Journal of Alloys and Compounds*, 617, (2014), 734–739.
- [7]. Bihui Li, Lijuan Luo, Ting Xiao, Xiaoyan Hu, Lu Lu, Jianbo Wang, Yiwen Tang Zn₂SnO₄-SnO₂ heterojunction nanocomposites for dye-sensitized solar cells, *Journal of Alloys and Compounds*, 509, (2011), 2186–2191.
- [8]. Davender Singh, Virender Singh Kundu, A.S. Maan Structural, morphological and gas sensing study of palladium doped tin oxide nanoparticles synthesized via hydrothermal technique, *Journal of Molecular Structure*, 1100, (2015), 562-569.
- [9]. R. Nurzulaikha, H.N. Lim, I. Harrison, S.S. Lim, A. Pandikumar, N.M. Huang, S.P. Lim, G.S.H. Thien, N. Yusoff, I. Ibrahim Graphene/SnO₂ nanocomposite-modified electrode for electrochemical detection of dopamine, *Sensing and Bio-Sensing Research*, 5, (2015), 42–49.
- [10]. Supphadate Sujinnapram and Sasimontong Mongsrijun Additive SnO₂-ZnO composite photoanode for improvement of power conversion efficiency in dye-sensitized solar cell, *Procedia Manufacturing*, 2, (2015), 108 – 112.
- [11]. Elaheh Kowsari, Mohammad Reza Ghezlbash Ionic liquid-assisted, facile synthesis of ZnO/SnO₂ nanocomposites, and investigation of their photocatalytic activity, *Materials Letters*, 68, (2012), 17–20.
- [12]. Chompoonuch Puchmark and Gobwute Rujjanagul The Effect of ZrO₂ Nanoparticles on Mechanical Property and Dielectric Respond of CaCu_{3.1}Ti₄O_{12.1} Ceramics, *Ferroelectrics*, 415, (2011), 101–106.
- [13]. G.N.Advani, A.G.Jordan, C.H.P.Lupis and R.L.Longini A Thermodynamic analysis of the deposition of SnO₂ thin films from the vapor phase, *Thin Solid Films*, 62, (1979), 361-368.
- [14]. Imran Khan, Shakeel Khan, Wasi Khan Temperature-dependent dielectric and magnetic properties of Mn doped zinc oxide nanoparticles, *Materials Science in Semiconductor Processing*, 26, (2014), 516–526.
- [15]. A.R. Babar et al Electrical and dielectric properties of co-precipitated nanocrystalline tin oxide, *Journal of Alloys and Compounds*, 505, (2010), 743–749.
- [16]. Edgar Mosquera, Carolina Rojas-Michea, Mauricio Morel, Francisco Gracia, Víctor Fuenzalida, Ramón A. Zárate Zinc oxide nanoparticles with incorporated silver: Structural, morphological, optical and vibrational properties, *Applied Surface Science*, 347, (2015), 561–568.
- [17]. J. M. Ramos, A. W. Carbonari, T. Martucci, M. S. Costa, G. A. Cabrera-Pasca, M. A.V. Macedo Jr, R. N. Saxena A weak magnetism observed in SnO₂ doped with Fe by means of Perturbed Gamma-Gamma Angular Correlation and Mössbauer Spectroscopy *Physics Procedia* ,28, (2012), 90 – 94.
- [18]. Adawiya J. Haider ,Suaad .S.Shaker & Asma H.Mohammed A study of morphological, optical and gas sensing properties for pure and Ag doped SnO₂ prepared by pulsed laser deposition (PLD) *Energy Procedia* , 36, (2013), 776 – 787.
- [19]. H. Lee , S.H. Park , S.J. Kim , Y.K. Park , B.H. Kim , S.C. Jung Synthesis of tin and tin oxide nanoparticles using liquid phase plasma in an aqueous solution , *Microelectronic Engineering* ,126 , (2014), 153–157.
- [20]. Marion Winkelmann, Eva-Maria Grimm, Talita Comunian, Barbara Freudig, Yunfei Zhou, Wolfgang Gerlinger, Bernd Sachweh, Heike Petra Schuchmann, Controlled droplet coalescence in miniemulsions to synthesize zinc oxide nanoparticles by precipitation, *Chemical Engineering Science*, 92, (2013), 126–133.
- [21]. S. Saednia, P. Iranmanesh, M. Hatefi Ardakani, M. Mohammadi, Gh. Norouzi, Phenoxo bridged dinuclear Zn(II) Schiff base complex as new precursor for preparation zinc oxide nanoparticles: Synthesis, characterization, crystal structures and photoluminescence studies, *Materials Research Bulletin*, 78, (2016), 1–10.
- [22]. L.A. Patil, I.G. Pathan, D.N. Suryawanshi, A.R. Bari, and D.S. Rane, Spray pyrolyzed ZnSnO₃ nanostructured thin films for hydrogen sensing *Procedia Materials Science*, 6, (2014), 1557 – 1565.
- [23]. Alireza Khataee, Behrouz Vahid, Shabnam Saadi, Sang Woo Joo, Development of an empirical kinetic model for sonocatalytic process using neodymium doped zinc oxide nanoparticles, *Ultrasonics Sonochemistry*, 29, (2016), 146–155.
- [24]. Lianmeng Zhang , Junyan Wu, Fei Chen, Xueping Li , Julie M. Schoenung, Qiang Shen Spark plasma sintering of antimony-doped tin oxide (ATO) nanoceramics with high density and enhanced electrical conductivity, *Journal of Asian Ceramic Societies*, 1 , (2013), 114–119.
- [25]. Yusuf Osman Donar, Ali Sina Catalytic effect of tin oxide nanoparticles on cellulose pyrolysis, *Journal of Analytical and Applied Pyrolysis*, 119, (2016), 69–74.

- [26]. N.M. Shaalan , D.Hamad, A.Y.Abdel-Latief, M.A.Abdel-Rahim Preparation of quantum size of tin oxide: Structural and physical characterization, *Progress in Natural Science : Materials International*, 26 , (2016), 145–151.
- [27]. Xiaojuan Wu, Zhiqiang Wei, Lingling Zhang, Xuan Wang, Hua Yang and Jinlong Jiang Optical and Magnetic Properties of Fe doped ZnO Nanoparticles obtained by Hydrothermal Synthesis, *Journal of Nanomaterials*, vol 2014, (2014), 6 pages.
- [28]. Numan Salah , Waleed M. AL-Shawafi , Sami S. Habib, Ameer Azam, Ahmed Alshahrie Growth-controlled from SnO₂ nanoparticles to SnO nanosheets with tunable properties, *Materials and Design*, 103, (2016), 339–347.
- [29]. G. Caputo, S.G. Leonardi, S. Mariotti, M. Latino, N. Donato, S. Trocino, N. Pinna, G. Neri Microstructural, electrical and hydrogen sensing properties of F-SnO₂ nanoparticles, *Procedia Engineering* ,87, (2014), 1087 – 1090.
- [30]. Asama. N. Naje , Azhar S. Norry, Abdulla. M. Suhail, Preparation and Characterization of SnO₂ Nanoparticles, *International Journal of Innovative Research in Science, Engineering and Technology*, Vol. 2, Issue 12, (2013), 7068-7072.
- [31]. Niti Yongvanich, Patama Visuttipitukkul, Waranya Assawasilapakul, Warunee Srichan and Siriporn Onlamoon Processing and Sintering of Zn_{0.92}Sn_{0.04}Bi_{0.02}Co_{0.02}O_β Nanopowders, *Energy Procedia*, 9, (2011), 498 – 508.
- [32]. Chien-Tsung Wang, Miao-Ting Chen, De-Lun Lai Surface characterization and reactivity of vanadium–tin oxide nanoparticles, *Applied Surface Science*, 257, (2011), 5109-5114.
- [33]. K.J.Abhirama, K.U.Madhu Electrical Parameters of (SnO₂)_{1-x}(ZnO)_x Nanocomposites Prepared By Solvothermal Method, *International Journal of Advance Engineering and Research Development (IJAERD)*, Volume 4, Issue 9, (2017), 511-518.
- [34]. Karzan Abdulkareem Omar, Bashdar Ismael Meena, Srwa Ali Muhammed Study On The Activity Of ZnO-SnO₂ Nanocomposite Against Bacteria And Fungi, *Physicochem. Probl. Miner. Process*, 52(2), (2016), 754–766.
- [35]. T.Larbi, B.Ouni, A.Boukachem, K.Boubaker, M.Amlouk Electrical measurements of dielectric properties of molybdenum-doped zinc oxide thin films, *Materials Science in Semiconductor Processing* , 22, (2014), 50–58.
- [36]. S. Tewari, A. Ghosh and A. Bhattacharjee Studies on frequency dependent electrical and dielectric properties of sintered zinc oxide pellets: effects of Al-doping, *Indian J Phys*, 0858-1, (2016), 9 pages.
- [37]. A.S.Lanje et al Dielectric study of tin oxide nanoparticles at low temperature, *Archives of Applied Science Research*, 2(2), (2010), 127-135.